International Journal of Engineering Research & Technology (IJERT)
ISSN: 2278-0181
Vol. 6 Issue 12, December - 2017

Simulation of Cracks Development due to Rebar Corrosion in the Cement Paste Ring

Eng. Lwitiko Humphrey Kalenga
Department of Structural and Construction Engineering,
College of Engineering and Technology,
University of Dar es salaam
Dar es salaam, Tanzania

***Abstract*- Corrosion of reinforced concrete structure causes cracks in the concrete, reduces the cross-section area of the reinforcement hence reduces the service life performances of the structures. The major cause of corrosion is a porous zone at the interface of rebar and concrete which is due to poor compaction, high porosity and high bleeding at the Interfacial Transition Zone (ITZ) of reinforcement and Concrete. The compaction of concrete via reinforcement i.e., Rebar shaking has proved to improve the compaction and to reduce porosity at ITZ because it increases bond and adhesion of rebar and concrete. In this technique of compaction the rebar is enveloped by fine particles i.e., it creates what can be characterized as Cement Paste Ring (CPR) around rebar. The concrete with CPR is being studied to see its suitability in protecting reinforcement from corrosion in Reinforced Concrete Structure. Cracks mechanism and behavior of concrete samples with CPR are compared with normal vibrated concrete samples (samples without CPR). A Pull-out test and a Hydraulic Concrete cracking machine were used to test the samples of different strengths and ages. Maturity Pull out tests show that cracks on the samples with CPR are less wide and the cracks pattern are disconnected as compared to normal vibrated samples of which its cracks are wider, and well-connected. The pull-out force is higher in samples with CPR than in normal vibrated samples. In the Hydraulic machine the samples with CPR showed more resistance in lateral pressure as compared to normal vibrated samples. Inner layer of samples with CPR formed a single continuous cracks which are vertically inside but diagonally outside. The normal vibrated samples displayed multiple vertical cracks inside and outside the samples. Micro-cracks were not visible (except by magnifiers) in samples with CPR but were clearly visible in normal vibrated samples. The cracks patterns, sizes, spacing as well as the bond strengths between rebar and concrete at ITZ have significance effect on the corrosion and crack mechanisms. From the experiments and analysis, the samples with CPR are promising to reduce corrosion on the reinforcement structure as compared to normal vibrated samples.**

Keywords—Corrosion, Cracks, Cement Paste Ring, Cover, ITZ

I. INTRODUCTION

Corrosion of reinforcing steel in concrete results in the formation of corrosion products at the surface of the reinforcing bar which leads to cracking and spalling of concrete cover. Corrosion reduces the cross-section area of the reinforcement hence decreases its tensile capacity and services life performances of the structure. Corrosion cracking and its related pressure have widely been studied by (Wang and Liu 2008, Ahmad, 2003, Yuan and Ji 2009, Zheng et al. 2005, Tamer and Khaled 2007, Chang et al. 2010). The expansion of corrosion products impose an internal radial pressure to radial surrounding concrete which leads to cracks at the point where exerted tensile forces is greater than the tensile strength of concrete.

A number of experimental studies, field and theoretical investigations have been conducted on radial expansion of corroded reinforcement, concrete cracking and bond interaction. The studies also tried to explain the mechanism of corrosion cracking (Bazant 1979, Andrade and Alonso 1996, Atimatay & Ferguson 1973, Beeby 1983). The cracking mechanism due to the corrosion effect on structural serviceability are still ongoing (e.g. Bhargava et al. 2005)

Studies about cracking mechanisms have been carried out through visual observation, using finite element models, accelerated corrosion tests, simulated corrosion tests and current studies are focusing on using fracture mechanisms (Du et al. 2005, Bohner and Brohl 2010).

A. Background

Poor compaction, high porosity and bleeding at Interfacial Transition Zone (ITZ) of steel and concrete are the major factors for accelerating corrosion. Therefore good compaction at ITZ reduce porosity and bleeding. The Rebar shaker is proposed to enhance good bond between rebar and concrete. Rebar Shaking is a process of turning rebar into a vibrator (Bennet et al. 2003). This practice leaves steel bars enveloped by cement paste which is regarded as a cement paste ring (CPR). The ongoing studies have shown that CPR reduces porosity at ITZ, and at the interface of cement paste and bulk concrete, it eliminates bleeding, and from pull-out tests results the bond strength between the rebar and CPR is significantly improved. Thus CPR is potential for controlling corrosion

Corrosion products are expansive and have greater volume than the initial steel. This induces corrosion cracking when the resulting tensile stress in the surrounding concrete reaches the tensile strength limit of concrete. Cracking occurs once the maximum hoop tensile stress exceeds the tensile strength of concrete. The cracking begins at the steel – concrete interface and propagates outwards and eventually result in the cracking of the cover concrete and this would indicate the loss of life for the corrosion affected structures

International Journal of Engineering Research & Technology (IJERT)
ISSN: 2278-0181
Vol. 6 Issue 12, December - 2017

(Bhargava et al., 2006, Capozucca 1995). The adequate prediction of the crack mechanisms, crack propagation and failure mechanism need to be investigated. The study used hydraulic machine to simulate corrosion pressure that induce cracks in order to study the cracking mechanisms of at ITZ of CPR and rebar together with the bulk concrete

II. EXPERIMENTS AND RESULTS

Two different types of concrete samples were used; one vibrated normally denoted as VIB and the other vibrated using a Rebar Shaker that produced a CPR layer, denoted as RS. A Pull-out test and a Hydraulic Concrete cracking machine were used to test the samples

A. pull out test

The tests were performed on both the reinforced concrete cylinder (RCC) samples shown in Figure I to determine their behavior. The sample details are shown on Table I.

Table I: SAMPLE DETAILS

Sample Type and Notation.	No. of Samples	Dimensions H*D (mm)	Average Gross weight. (kg)	Bar Diameter (mm)	Curing history	Average vibration time (s)
Vibrated with REBAR SHAKER MACHINE (RS).	3	300*150	13.799	16	14 days at 20°C	30
Vibrated Normally (VIB).	3	300*150	13.802	16	14 days at 20°C	30

I. Sample Testing and Results Compilation.

After 14 days of curing, the samples were tested using Pull out test machine and the results and observations are as shown in Tables II (a, b)

Figure 1: Concrete cylindrical samples (RS and VIB) after 14 days of curing.

TABLE II (a): PULL OUT TEST RESULTS

Type of samples	Sample notation	Applied max. force (KN)	Failure type	Number of visible cracks (as viewed from the top of the sample only)
RS samples	S_0	135	Steel Rebar failure/broken	5
	S_1	131	Steel Rebar failure	4
	S_2	129	Steel Rebar failure/deformed	3
VIB samples	S_0	122	Rebar pulled out + sample failure/splits	5
	S_1	101	Rebar pulled out + sample splits in two.	3
	S_2	115	Rebar pulled out + sample failure	3

From Table II (a) failure behavior revealed some interesting crack patterns. The samples were studied closely, observations were recorded in Table II (b).

International Journal of Engineering Research & Technology (IJERT)
ISSN: 2278-0181
Vol. 6 Issue 12, December - 2017

TABLE II (b): CRACK OBSERVATIONS

Sample Type	Sample Notation	Crack Width (mm)	No. visible cracks	Failure Type (direction)	Penetration.	Crack Patterns.
RS sample	S_0	C_1=0.14	5	From Rebar to the rest of the concrete	Deep penetration for C_1 shallow for the rest.	Formed a radial pattern around the rebar
		C_2=0.18				
		C_3=0.04				
		N_1 =0.08		From concrete cover towards the rebar.	Short and shallow	Radially around concrete cover/perpendicular to the rebar.
		N_2 =0.04				
	S_1	C_1=0.08	4	From Rebar to the rest of the concrete.	Deep penetration for C_2 shallow for the rest.	Formed a radial pattern around the rebar
		C_2=0.18				
		N_1=0.1		From concrete cover towards the rebar.	All short and shallow	Radially around concrete cover/perpendicular to the rebar.
		N_2=0.28				
	S_2	C_1=0.06	3	From Rebar to the rest of the concrete	Deep C_2 and C_1 short shallow	Formed a radial pattern around the rebar with minor diagonal micro cracking.
		C_2=0.1				
		N=0.02		From concrete cover towards the rebar.	Short and shallow	Radially around concrete cover/perpendicular to the rebar.
VIB sample	S_0	C_1=1.8	3	Cut though the sample.	Deep through the sample.	Perpendicular to the rebar.
		C_2=0.2		From Rebar to the rest of the concrete	Short and shallow.	Randomly distributed, some diagonal.
		C_3=0.1				
	S_1	C_1=2.2	5	Cut though the sample/continuous to both sides.	Deep through the sample.	Perpendicular to the rebar.
		C_2=0.2				
		C_3=0.7		From Rebar to the rest of the concrete	Short and shallow.	Randomly distributed, some diagonal.
		C_4=0.06				
		C_5=0.08				
	S_2	C_1= through	3	Total sample failure/sample split.	Cut though the sample.	Perpendicular to the rebar.
		C_2=0.8		From Rebar to the rest of the concrete	Short and shallow.	Randomly distributed, some diagonal.
		C_3=1.2				

NB: **C** = Stands for cracks originating from the rebar, **N** = Stands for cracks originating from the concrete cover.

International Journal of Engineering Research & Technology (IJERT)
ISSN: 2278-0181
Vol. 6 Issue 12, December - 2017

Figures 2 and 3 are photos of the concrete samples after the test was conducted

Figure 2: RS concrete samples showing visible cracks after the test

Figure 3: VIB concrete samples showing failure patterns and some visible cracks

After detailed observation and study of the tested samples, some remarks where reached as follows:

i. It was observed that cracks formed on the RS sample are less wide from Table II (b) and form a clearer and disconnected cracks patterns around the reinforcement.

ii. The RS samples form a non-continuous network of micro cracks (cracks), unlike normal vibrated (VIB) samples as shown in Figure 4 (a and b)

iii. From Table II (a) above the RS samples resisted more pull-out force compared with the normally vibrated sample (VIB), and this shows that its bond has an increased bonding strength than the normal vibrated reinforced concrete bond.

iv. Crack widths for RS samples are ranging from 0.02 to 0.28mm and for VIB samples crack widths are ranging from 0.08 to 1.8mm.

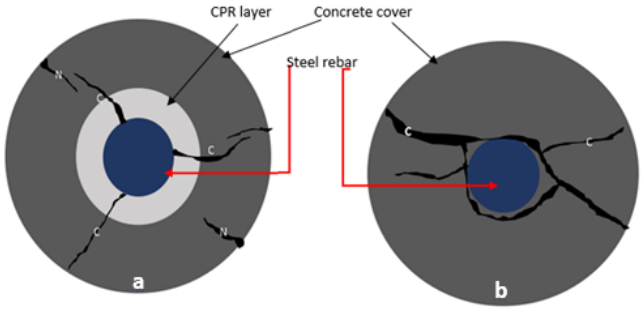

Figure 4: Schematic of the crack pattern in RS sample (a) and VIB sample (b)

B. Hydraulic Concrete Cracking Machine

The machine was used mainly to induce the internal lateral pressure to the inner concrete layer that forms the bond with the steel rebar, and also to induce stresses in concrete similar to effects created by the corrosion around the rebar (lateral expansion) hence causing cracks on the cover. The machine contains different parts such as the pressure gauge for measuring lateral pressure subjected to the concrete samples as shown in Figure 5.

The machine operates under hydraulic laws. Hydraulic fluid is pumped into the concrete sample with the aid of the hand pump attached to the pressure gauge which records the amount of pressure conveyed. The machine contains different parts as listed below:

1. Top plate; 2. Hydraulic hand pump; 3.Vertical bolts; 4. Safety case; 5. Hydraulic delivering nozzle; 6. Hydraulic pipe; 7. Pressure gauge.

Figure 5: Hydraulic concrete cracking machine

Following the requirements of the machine, the samples were prepared by replacing the steel rebar with the PVC pipe which was later pulled out after concrete setting leaving the hollow space in the middle of the concrete cylinder and exposing the inner layer, as shown in Figure 6 and sample details are shown in Table III

International Journal of Engineering Research & Technology (IJERT)
ISSN: 2278-0181
Vol. 6 Issue 12, December - 2017

Figure 6: Samples with PVC immediately after preparation and without PVC pipe after setting.

TABLE III: CONCRETE SAMPLE DETAILS

Sample type and Notation	No. of Samples	Dimensions H*D (mm)	Average Gross weight. (kg)	PVC Diameter (mm)	Curing history	Average vibration time (s)
Vibrated with REBAR SHAKER MACHINE (RS).	3	300*150	13.099	18	07 days at 20°C	45
Vibrated Normally (VIB).	3	300*150	13.002	18	07 days at 20°C	45
Vibrated with REBAR SHAKER MACHINE (RS).	2	300*150	13.01	18	28 days at 20°C	45

I. Testing Procedures and Results

After effective curing, the samples were removed and left to dry at room temperature for 72 hours and then put into the machine by inserting the hydraulic delivering nozzle in the hollow part of the sample. Then, the sample was secured on the machine by tightening the bolts and by using the hand pipe the hydraulic fluid was pumped into the sample hence creating the pressure inside the sample until failure was detected as shown in Figure 7. The failure was due to the development of cracks on the side(s) of the samples as well as the top, as shown in Figure 8

Figure 7: Sample under testing

Figure 8: Cracked sample after testing.

Following a series of tests of the samples (both 7days and 28 days old), the initial test results are as shown in Table IV(a) and (b) and thorough observations on the failure type of the samples were done concentrating much on the cracks patterns, width and other parameters.

International Journal of Engineering Research & Technology (IJERT)
ISSN: 2278-0181
Vol. 6 Issue 12, December - 2017

Table IV (a): FAILURE TYPE OF THE SAMPLES (7 DAYS AGE)

Sample Types	Sample number	Applied lateral pressure (Kg/cm2)	Failure type
RS samples	S1	95	Visible lateral side and top side cracks – escape of fluid from top and lateral sides of the sample.
	S2	105	Visible lateral side and top cracks – escape of fluid from top and lateral side of the sample.
	S3	100	Visible one lateral side and top cracks – escape of fluid from top and lateral side of the sample.
VIB samples	S1	85	Visible lateral side and top cracks – escape of fluid from both lateral sides of the sample.
	S2	65	Visible lateral side and top cracks – escape of fluid on both sides of the sample.
	S3	75	Visible lateral side and top cracks – escape of fluid from one lateral side of the sample.

From Table IV (a) the average applied lateral pressure was 100 kg/cm2 and 75 kg/cm2 for RS samples and VIB samples respectively. The RS samples showed more resistance in lateral pressure, this is due to impermeability property of the CPR layer in contact with the hydraulic pressure. It is advantageous that this layer would resist the pressure caused by the formation of rust (corrosion) which may increase durability hence life span of the concrete.

The tests were carried out on 14 days old, RS samples as recorded in the following Table IV (b)

Table IV (b): FAILURE TYPE OF THE SAMPLES (28 DAYS AGE) ON RS SAMPLES

Sample Type	Sample number	Applied lateral pressure (Kg/cm^2)	Failure type
RS samples	S1	145	Visible one lateral side and top side cracks – escape of fluid from top and side of the sample.
	S2	160	Visible one lateral side and top cracks – escape of fluid from top and side of the sample.
Average		152.5	

The Table IV (b) showed an increased pressure for the 28 days old cured samples with an average pressure of 152.5 kg/cm2. By using the concrete crack meter (magnifier) as seen in the Figure 9 below the cracked samples where studied and observed as recorded in the Table V.

Figure 9: Observation of crack widths using crack meter

International Journal of Engineering Research & Technology (IJERT)
ISSN: 2278-0181
Vol. 6 Issue 12, December - 2017

TABLE V: CRACKS OBSERVATIONS FOR THE SAMPLES (7 DAYS AGE)

Sample Type	Sample ID	Top side		Lateral sides	
		width	Pattern type	width	Pattern type
RS samples	S1	C_s/C_e = 0.16/0.11	From the concrete center towards the concrete cover by forming tributaries like shape at the start.	S_1= 0.08	Short and Diagonal pattern running from top of the sample up to the middle.
		C_s/C_e = 0.14/0.18	Short, less straight, non-continuous running from the center towards the cover end.	S_2 = 0.1	
	S2	C_s/C_e = 0.2/0.14	Short, less straight, non-continuous running from the center towards the cover end	S_1=0.04	Series of short and Diagonal pattern running from top of the sample up to the middle.
		C_s/C_e = 0.28/0.18		S_2=0.02	
	S3	C_s/C_e = 0.18/0.1	Short, less straight, non-continuous running from the center towards the cover end	S= 0.2	Short and Diagonal pattern running from top of the sample up to the middle.
		C = 0.1			
VIB samples	S1	C_s/C_e =0.3/0.2	Multiple continuous cracks, running from the center towards the cover end.	S_1=1.4	Vertical, continuous running longitudinally from the top to bottom of the sample.
		C_s/C_e= 0.2/0.18		S_2=0.4	
		C= 0.18			
	S2	C_s/C_e= 0.28/0.06	Two continuous, straight cracks	S_1=0.2	Vertical, continuous running longitudinally from the top to
		C_s/C_e = 0.2/0.08		S_2=0.04	
	S3	C_s/C_e = 0.2/0.18	Multiple continuous cracks from center to cover end, one short cracks originating from the cover end.	S_1=0.12	Vertical, deep, continuous running longitudinally from top to bottom of the sample.
		C_s/C_e = 0.18/0.08		S_2=0.8	
		C = 0.8		S_3=0.08	

International Journal of Engineering Research & Technology (IJERT)
ISSN: 2278-0181
Vol. 6 Issue 12, December - 2017

TABLE VI: CRACKS OBSERVATIONS FOR RS SAMPLES (28 DAYS AGE)

Sample Type	S/N	Top side		Lateral sides	
		width	Pattern type	width	Pattern type
RS Samples	1	C_s/C_e = 0.3/0.2	One continuous, zigzag, from center to the end cover. Other short and non-continuous.	S_1=0.8	Vertical short cracks running from top to half the height of the sample.
		C_s/C_e = 0.2/0.04		S_2=0.1	
				S_3=0.06	
	2	C_s/C_e = 0.38/0.8		S_1=0.6	Vertical short cracks running from top to half the height of the sample.
		C_s/C_e = 0.3/0.08		S_2=0.04	

NB: C_S/C_e signifies crack width at the start and end of the crack and S_n signifies with of side cracks where by n stands for number of cracks.

Cracks observations for the samples shown in Figure 10 were done at the top, side surfaces and in the inner surfaces as shown in Figure 11

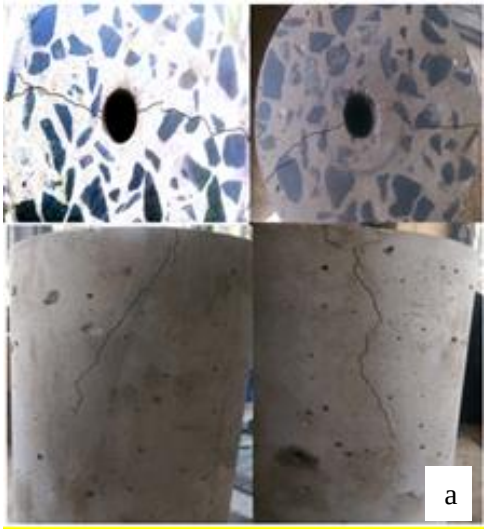

Figure 10: RS samples in (a) and VIB samples in (b) showing top surfaces and side cracks

Cracks observations were done; visually and micro cracks were observed using crack meter magnifier. It was observed that:

i. Inner layer of the RS samples formed a single continuous cracks as shown in Figure 11(a), some short some long running vertically, to the outer sides (diagonally) cracks as seen in Fig 10(a)

ii. The inner layer of the VIB samples displayed multiple vertical cracks extending the whole depth of the sample shown in Figure 11(b), which are straight on the outside with some branches of continuous cracks

iii. Typical Micro-cracks patterns of RS sample in Figure 12(a) and VIB sample in Figure 12(b). The continuous longitudinal crack is visible

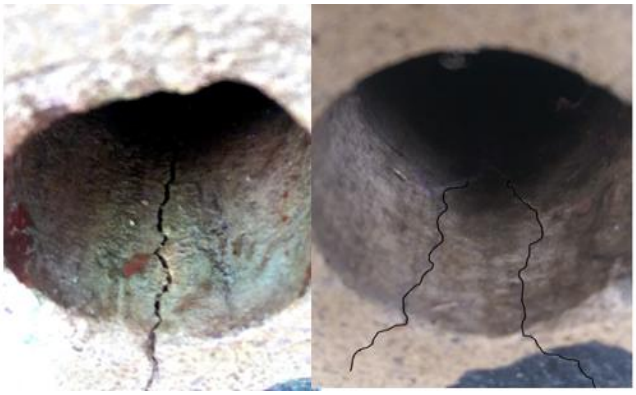

Figure 11: RS sample general pattern for both 7&28 days and VIB inner layer cracks

International Journal of Engineering Research & Technology (IJERT)
ISSN: 2278-0181
Vol. 6 Issue 12, December - 2017

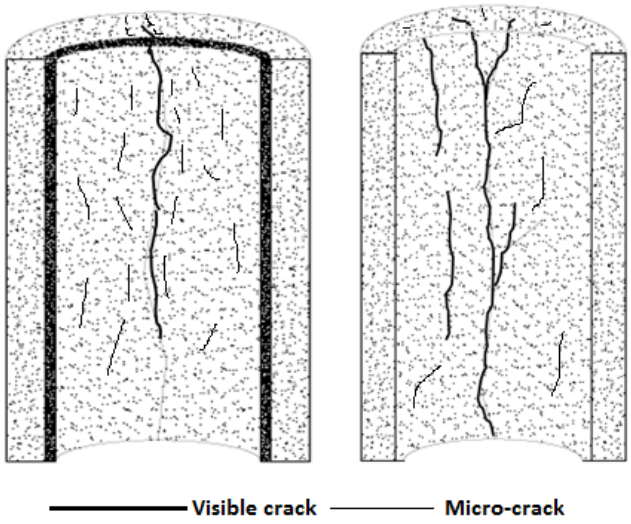

(a) (b)

Figure 12: Micro-cracks patterns of inner surface walls of the RS sample on the left and VIB sample on the right

The visible inner cracks in the RS samples had widths from 0.1 to 0.22 mm and with micro crack meter cracks of 0.005 to 0.01mm were observed, lengths of localized interconnected cracks varied from 0.5 to 30mm, the longest inner longitudinal crack (which was 90mm long) had widths varying from 0.22 to 0.4mm. The VIB samples had widths varying from 0.28 to 0.5mm and micro crack meter observed cracks of 0.009 to 0.05mm, the length of localized interconnected cracks varied from 0.9 to 40mm, the longest inner longitudinal crack had width of 0.7mm. Unlike the RS, the VIB internal crack had a similar shape with the outside. One part of longitudinal crack in the VIB sample, other two or three radial cracks with length of about 40mm and inclined between 40 to 80 degrees to the main crack were formed. For RS samples inside cracks were vertically straight but externally the cracks were inclined from top to bottom. The crack widths conformed to the results of various researches that have been done in corrosion induced crack widths (Otieno et al., (2006), Katrien et al., 2009, Schiessl and Raupach (1997), Berke et al., (1993), Moreno and Rourke (2008)).

III. DISCUSSION OF RESULTS

The pullout tests results in Table II (b) show that crack widths formed in the RS samples are smaller as compared to VIB samples; the cracks are straight due to the existence of well compacted particles which increase the confined stress thus increasing bond strength. The RS samples form a non-continuous network of micro cracks, unlike normal vibrated (VIB) samples which is beneficial in combating corrosion. This is brought about by the existence of different properties between the CPR layer and the concrete cover as shown in Figure 3. The bond between CPR and rebar is higher and well improved as compared to normally vibrated samples. The increased bond has an impact on the mechanism of cracking as compared to the normal vibrated samples. Furthermore, in Figure 4, it is seen that the crack from rebar to the cover is not continuous in RS samples but they are continuous in VIB samples. Thus ingress of harmful chemicals is easy in VIB samples but they are intervallic in RS samples. Crack widths for RS samples range from 0.02 to 1.2mm and for VIB samples are range from 0.08 to 1.8mm.The crack propagation and widths is influenced by the bond strengths and type of materials at the interfacial transition zone between reinforcement and concrete and size of reinforcement. The cracks spacing are closer and shorter in RS samples as compared to the VIB samples (Ghali et al. 2002)

When using the hydraulic cracking machine, the average applied radial pressure was higher for RS samples by 25% more than for VIB samples. The RS samples showed more resistance in lateral pressure, due to compatibility and impermeability properties of the CPR layer in contact with the hydraulic pressure. Inner layer of the RS samples formed a single continuous crack, some short some long running vertically, contrary to the outer sides (diagonally) cracks, this is due to the consistency, and existence of well compacted CPR hence increased resistance for cracking. The inner layer of the VIB samples displayed multiple vertical cracks running the whole depth of the sample as shown in Figure 12.

The hydraulic pressure exerts an outward pressure on the concrete similar to corrosion products. After cracking initiation at the interface of rebar and CPR, the crack in the concrete cylinder propagates along a radial direction and held at the interface between CPR and bulk concrete. The CPR is considered as a cracked zone and bulk concrete considered as un-cracked, because of the differences of moduli between CPR and bulk concrete, modulus and stiffness of CPR are lower compared to the bulk concrete. The initiated and propagated cracks which have stuck at the interface of CPR and bulk concrete tend to join up and initiate other new cracks on the bulk concrete. The random nature of cracks occurrence which occur simultaneously at the inner part of the cylinder and for a short period of time, the similar nature of cracks was also explained by (Li et al. 2005)

It is obvious that the cracking of concrete cover is the direct consequence of an increasing radial expansion of corroded reinforcement. Internal cracking is always initiated at the location of the maximum expansion and external cracking always initiated where the cover is a minimum (Du et al. 2006). Cracks occur first on the internal surface of the concrete cover at the point where the maximum radial expansion is experienced, because of the strong bond of CPR on the rebar, the point of maximum tensile stress cannot be at one point at various points, which explain why initiation of cracks occur at higher stresses compared to the propagations of cracks. It should also be noted that the failure of bulk concrete (cover) depends on strength of the paste, coarse aggregate, and the paste-aggregate interface. This interface is normally the weakest region of concrete and is where failure occurs before its occurrence on the aggregate or the paste (Vervuurt 1995). The ITZ between CPR and bulk concrete is well compacted and is another hardest layer to get cracked compared to the ITZ between rebar and CPR.

International Journal of Engineering Research & Technology (IJERT)
ISSN: 2278-0181
Vol. 6 Issue 12, December - 2017

As the radial expansion increases, more cracks occur on the internal surface of the cylinder and then propagate outwards. Before these cracks penetrate the cylinder, the first cracks appear on the external surface of the cylinder at the location where the micro cracks are concentrated more than any other points on the cylinder. First cracking that appear on the external side of the cylinder is referred to as external cracking. Once external crack appears, the internal stresses relax, which stops the propagation of other internal cracks (Nguyen et al. 2006). This is also the time for corrosion products to fill these cracks, hence to limit production of more corrosion products.

Zhang et al. 2009 depicts that at the initiation of corrosion cracking, the corrosion cracks are always short and very narrow, which limits the access of aggressive agents to the steel bars. In the secondary stage of corrosion development, the longitudinal corrosion cracks interconnect and grow wider. This leads to further steel–concrete interface to be exposed. In CPR, observations are a bit different; the steel-concrete interface is not exposed as the micro cracks accommodate corrosion products but also the CPR is of fine particles which gives room for fine particles to detach and become isolated thus increase protection in the reinforcement. External cracking is a results of interconnected longitudinal cracks, which tend to be wider than inside hence causing spalling.

Unlike other studies e.g., Bhargav et al. (2005) which indicated the presence of porous zone at the ITZ of steel and the concrete, the presence of CPR assumes that the porous zone is non-existence. Furthermore, the gradual filling of porous zone with the corrosion products does not pose pressure to the concrete until the porous zone is completely filled. The crack at CPR together with filled corrosion products both get stuck at the ITZ of CPR and bulk concrete, increase of rust materials creates more cracks at the CPR zone. When all micro-cracks are filled another considerable amount of cracks and corrosion products are needed to create new cracks on the bulk concrete. This phenomenon decrease corrosion rates and restrict increase of rust materials hence beneficial in combating corrosion. Ghali (2002) depicted that crack width depends mainly on the stress in steel after cracking, bond properties of the bars, properties of concrete and the shape of strain distribution which are applicable in RS samples which have CPR.

The maximum time from applying hydraulic pressure to the RS sample which has CPR until the occurrence of external crack is between 80 seconds to 120 seconds. Typical graph of Crack width versus Time is shown in Figure 13. It takes approximately 10 second for pressure to build-up until the first crack to appear. This nature of graphs is conforming to the results of Crack width versus Time that was done by Dimitri et al. (2009)

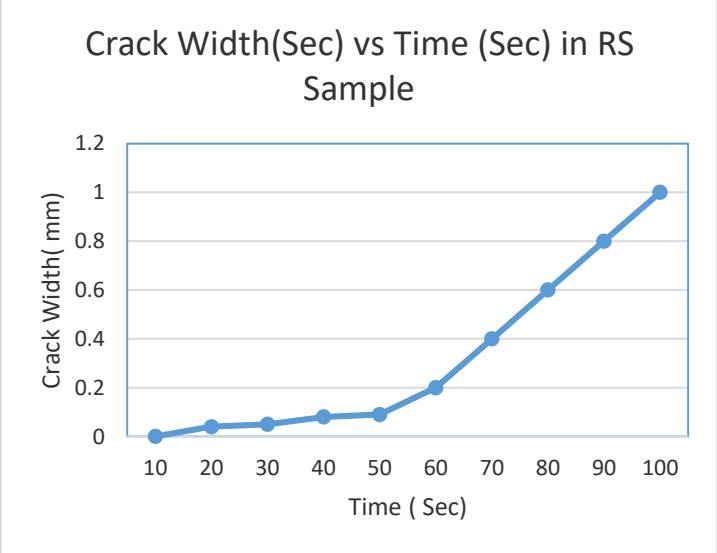

Figure 13: Crack widths vs. Time for RS samples

IV. CONCLUSIONS

From the study carried out, the following are the conclusions.

i. The Pressure needed to cause crack in the concrete samples that have Cement Paste Ring (CPR) as a result of Rebar shaked is higher than in the normal vibrated concrete samples
ii. Crack widths are thinner and shorter in CPR samples than in the normal vibrated samples. Also cracks spacing are closer and shorter in CPR samples as compared to the normal vibrated samples.
iii. The CPR is considered as a cracked zone and bulk concrete considered as un-cracked because of the differences of moduli between CPR and bulk concrete. Modulus and stiffness of CPR are lower compared to the bulk concrete and CPR experience more pressure as compared to the rest of the concrete
iv. The cracks in the CPR samples are not continuous from inner to the outer of the samples as compared to the normal vibrated samples which are continuous.
v. A great number of cracks formed in the inner surfaces of CPR do not align with the outer cracks showing no continuation of cracks which is due to the existence of the hardest layer at ITZ between CPR and bulk concrete, the stress is building up at this zone hence starts new pattern of crack in bulk concrete.
vi. The bond between CPR and rebar is higher as compared to the normal vibrated samples, and this has an influence on crack widths and pattern

International Journal of Engineering Research & Technology (IJERT)
ISSN: 2278-0181
Vol. 6 Issue 12, December - 2017

V. RECOMMENDATIONS

In order to have more knowledge of cracks and CPR zone, the strain behavior of the samples in relation to the pressure caused need to be studied further.

REFERENCES

[1] Ahmad, S., (2003), "*Reinforcement corrosion in concrete structures, its monitoring and service life prediction—a review".* Journal of Cement & Concrete Composites (25), Volume 4, Elsevier Science press, Suite 1900, Atlanta, and pp 459–471.

[2] Andrade, C., Alonso, C., Rodriguez, J. & Garcia, M. (1996) Cover cracking and amount of rebar corrosion: importance of the current applied accelerated tests. *In concrete repair, Rehabilitation and protection*, R. K. Dhir and M. R. Jones eds., E&FN Spon, London, UK, pp. 263-273

[3] Atimatay, E. & Ferguson, M. (1973) ''Early corrosion of reinforced concrete – A test report'' *ACI Structural Journal*, 70, 9, pp. 606-611

[4] Bazant, Z. P. (1979) Physical model for steel corrosion in concrete sea structures – theory. *Journal Structural Division*, ASCE, 105, ST6, pp., 1137-1153.

[5] Beeby, A. W. 1983. Cracking, cover and corrosion of reinforcement. *Concrete International*, 5, 2, Pg. 35-40.

[6] Bennet, Richard; Randy Rainwater; Edwin Burdete., (2003), *"Testing of the Oztec/Rhodes Reinforcing Bar Shaker -Final Report.* The University of Tennessee, Department of Civil and Environmental Engineering Knoxville, Tennessee.

[7] Berke, N.S. M.P. Dellaire, M.C. Hicks, and R.J. Hoopes, "Corrosion of Steel in Cracked Concrete," Corrosion, Vol. 49, 1993, p. 934.

[8] Bhargava, K., Ghosh, A.K., Mori, Y. & Ramanujam, S. (2005) Modeling of time to corrosion-induced cover cracking in reinforced concrete structures. In *Cement and Concrete Research* 35, pp. 2203-2218

[9] Bhargava, K., Ghoshb, A.K., Yasuhiro, M., Ramanujama, C.S., (2006), *"Analytical model for time to cover cracking in RC structures due to rebar corrosion".* Nuclear Engineering and Design (23), Volume 6, Sao Paulo, pp 1123–1139.

[10] Bohner E, H.S. Müller & S. Bröhl (2010) Investigations on the mechanism of concrete cover cracking due to reinforcement corrosion. *Institute of Concrete Structures and Building Materials, Karlsruhe Institute of Technology, Germany. Fracture Mechanics of Concrete and Concrete Structures - Assessment, Durability, Monitoring and Retrofitting of Concrete Structures- B. H. Oh, et al. (Eds) © 2010 Korea Concrete Institute, Seoul, ISBN 978-89-5708-181-5*

[11] Capozucca Roberto (1995) Damage to reinforced concrete due to Reinforcement corrosion. *ISTC, University of Ancona, Facolth di Ingegneria, Via Brecce Bianche, 60131 Ancona, Italy*. Construction and Building Marerials, Vol. 9, No. 5, pp. 295-303, 1995 Copyright 8 1995 Elsevier Science Ltd Printed in Great Britain. All rights reserved; 0950-0618(95)00033-X; 09504618/95 510.00+0.00

[12] Chang, Che Way., Hung Sheng Lien., Chen Hua Lin., (2010),"*Determination of the stress intensity factors due to corrosion cracking in ferroconcrete by digital image processing reflection photo elasticity"*. Journal of Corrosion Science (52), Issue 5, Elsevier Press, Atlanta, pp 1570–1575.

[13] Dimitri V. Val, Leonid Chernin, Konstantin Y. Volokh (2009) ''Analytical modelling of concrete cover cracking caused by corrosion of reinforcement'' Received: 10 March 2008 / Accepted: 19 May 2009 / Published online: 26 May 2009 RILEM 2009 Materials and Structures (2010) 43:543–556 DOI 10.1617/s11527-009-9510-2

[14] Du, Y.G., A.H.C. Chan, L.A. Clark (2006) Finite element analysis of the effects of radial expansion of corroded reinforcement, Computers and Structures 84(2006) 917–929;

[15] Ghali, R. Favre, M. Elbadry (2002) Concrete Structures Stresses and Deformations, *British Library Cataloguing in Publication Data* A catalogue record for this book is available from the British Library, *Library of Congress Cataloging in Publication Data*, ISBN 0–415–24721– This edition published in the Taylor & Francis e-book

[16] Katrien Audenaert, Geert De Schutter1, Liviu Marsavina, Veerle Boel1., (2009) Influence of cracks and crack width on penetration depth of chlorides in concrete; Magnel Laboratory for Concrete Research; University "Politehnica" Timisoara, Department Strength of Materials, Romania. European Journal of Environmental and Civil Engineering Volume 13, 2009 - Issue 5, Pages 561-572 | Published online: 05 Oct 2011

[17] Li C.Q and W.Lawanwisut (2005)"Crack Width due to Corroded Bar in Reinforced Concrete Structures". International Journal of Materials & Structural Reliability Vol.3, September 2005, 87-94

[18] Moreno F.J. and D. Rourke (2008) "Towards Achieving the 100 Year Bridge Using Galvanized Rebar," paper presented at the International Corrosion Congress, Las Vegas, May

[19] Nguyen, Q. T., Millard, A., Care, S., L'Hostis, V., and Berthaud, Y. (2006). "Fracture of concrete caused by the reinforcement corrosion products." J. Phys. IV, 136, 109–120. Ohtsu, M., and Yosimura, S.

[20] Otieno, M. B, M. G. Alexander and H.-D. Beushausen., (2006), Corrosion in cracked and uncracked concrete – influence of crack width, concrete quality and crack reopening. Magazine of Concrete Research, 2010, 62, No. 6, June, 393–404 doi: 10.1680/macr.2010.62.6.393, University of Cape Town

[21] Schiessl P. and Raupach. M, (1997) "Laboratory Studies and Calculations on the Influence of Crack Width on Chloride-Induced Corrosion of Steel in Concrete," ACI Materials Journal, Vol. 94(1), p. 56.

[22] Tamer, El Maaddawy., and Khaled Soudki., (2007), *"A model for prediction of time from corrosion initiation to corrosion cracking."* Journal of Cement & Concrete Composites (29), Elsevier Press, pp 168–175.

[23] Vervuurt A., Van Mier J.GM, Chiaia B. (1995) 'Damage evolution in different types of concrete by means of splitting tests''. HERON Vol.40, No.4-ISSN 0046-7316

[24] Wang, Shu-chen Li., and Liu, Shu-cai., (2008),"*Model for cover cracking due to corrosion expansion and uniform stresses at infinity".* Journal of Applied Mathematical Modelling (32) pp 1436–1444.

[25] Yuan, Y., and Yongsheng Ji., (2009), *"Modeling corroded section configuration of steel bar in concrete structure"*. Construction and Building Materials (23), Elsevier Ltd, pp 2461–2466.

[26] Zhang Ruijin, Arnaud, Raoul François (2009) Concrete cover cracking with reinforcement corrosion of RC beam during chloride-induced corrosion process. Modern Design and Analysis Research Institute, Northeastern University, Shenyang, China b LMDC (Laboratoire Matériaux et Durabilité des Constructions), Université de Toulouse, UPS, INSA, Toulouse, France Cement and Concrete Research 40 (2010) 415–425

[27] Zheng, J.J., Li, C.Q., and Lawanwisut, W., (2005), *"Modeling of Crack Width in Concrete Structures Due to Expansion of Reinforcement Corrosion"* 10DBMC International Conférence On Durability of Building Materials and Components LYON [France] 17-20 April.